

Efficient p53 Activation and Apoptosis by Simultaneous Disruption of Binding to MDM2 and MDMX

Baoli Hu, Daniele M. Gilkes, and Jiandong Chen

Molecular Oncology Program, H. Lee Moffitt Cancer Center and Research Institute, Tampa, Florida

Abstract

The p53 tumor suppressor plays a key role in protection against malignant transformation. MDM2 and MDMX are important regulators of the transcriptional activity and stability of p53 by binding to its NH₂ terminus. Recent studies suggest that inhibition of both MDM2 and MDMX is necessary for robust activation of p53 in certain tumor cells. However, small-molecule MDM2 inhibitors such as Nutlin fail to inhibit MDMX despite significant homology between the two proteins. The therapeutic efficacy of such compounds may be compromised by MDMX overexpression. To evaluate the feasibility and biological effects of simultaneously disrupting p53 binding to MDM2 and MDMX, we used phage display to identify a novel peptide that can inhibit p53 interactions with MDM2 (IC₅₀ = 10 nmol/L) and MDMX (IC₅₀ = 100 nmol/L). Expression of a scaffold protein (thioredoxin) displaying this peptide sequence by adenovirus disrupts both MDM2 and MDMX interaction with p53, resulting in efficient p53 activation, cell cycle arrest, and apoptosis of tumor cells overexpressing MDM2 and MDMX. Intratumoral injection of the adenovirus also induces growth suppression of tumor xenografts in mice in a p53-dependent fashion. These results show the therapeutic potential of targeting both MDM2 and MDMX in cancer, and provide a novel structural motif for the design of potent p53 activators. [Cancer Res 2007;67(18):8810–7]

Introduction

MDM2 is a ubiquitin E3 ligase for p53 and an important regulator of p53 stability and activity by forming a negative feedback loop (1, 2). Overexpression of MDM2 abrogates the ability of p53 to induce cell cycle arrest and apoptosis (3). In ~30% of human osteogenic sarcomas and soft tissue sarcomas, MDM2 is overexpressed due to gene amplification. In tumors without *MDM2* amplification, hyperactivation of MDM2 due to silencing of ARF expression also leads to p53 inactivation. Therefore, MDM2 is a key factor in tolerance of wild-type p53 in nearly 50% of tumors, making it an attractive target for the development of novel antitumor agents (4).

The MDM2 homologue MDMX also binds to p53 and inhibits p53-dependent transcription (5). Loss of *MDM2* or *MDMX* leads to embryonic lethality, which can be rescued by deletion of *p53* (6–8). Therefore, expression of both MDM2 and MDMX is necessary for regulation of p53 during development. Unlike MDM2, MDMX does not have significant intrinsic E3 ligase activity (9). However, MDMX forms heterodimers with MDM2 through COOH-terminal RING

domain interactions, which stimulates the ability of MDM2 to ubiquitinate and degrade p53 (10–13). Another consequence of MDMX-MDM2 heterodimer formation is that MDMX can be ubiquitinated and degraded by MDM2 (14–16); this is an important mechanism for controlling MDMX level during p53 stress response.

Recent studies suggest that the major mechanism of p53 regulation by MDMX is the formation of inactive MDMX-p53 complexes. Under nonstress conditions, MDM2 and p53 have short half-lives whereas MDMX is relatively stable. Therefore, elimination of MDMX is important for efficient p53 activation during stress response. DNA damage induces MDMX phosphorylation by ATM and Chk2 at several COOH-terminal serine residues (Ser³⁴², Ser³⁶⁷, and Ser⁴⁰³) generating a docking site for 14-3-3. These modifications stimulate MDMX degradation by MDM2, which facilitates p53 activation (17–20). Ribosomal stress resulting from disruption of rRNA biogenesis also activates p53, in part, by promoting MDMX degradation through L11-MDM2 binding, which enhances MDMX ubiquitination (21–24). MDMX overexpression leads to sequestration of p53 into inactive complexes and abrogates p53-mediated cell cycle arrest in response to ribosomal stress (24).

MDMX overexpression has been found in 40% of tumor cell lines (25), and in breast, colon, and lung tumor samples with 18.5% frequency (26). It is amplified in 4% of glioblastomas (27) and 5% of breast tumors (26). More recently, ~60% of retinoblastomas have been found to have *MDMX* overexpression or gene amplification (28). *MDMX* overexpression prevents oncogenic *ras*-induced premature senescence in mouse fibroblasts and cooperates with activated *ras* to confer tumorigenic potential in nude mice (26). RNAi-mediated knockdown of *MDMX* in HCT116 tumor cells suppresses tumor xenograft formation in nude mice (24). Because *MDM2* and *MDMX* overexpression or deregulation mainly occurs in tumors that retain wild-type *p53*, they are appealing targets for cancer drug discovery.

The extensive validation of MDM2 as a drug target resulted in the development of Nutlin, which can activate p53 by disrupting MDM2-p53 complex in tumor cells and tumor xenograft models (29). MDM2 and MDMX showed ~50% amino acid sequence identity in their p53-binding domains. However, recent studies reveal that Nutlin is inefficient for disruption of MDMX-p53 interaction and failed to activate p53 in cells overexpressing MDMX (30–32). Knockdown of MDMX cooperates with Nutlin to activate p53 in tumor cells and induces growth arrest. These results suggest that development of novel inhibitors optimized for dual-inhibition of MDM2 and MDMX is necessary to achieve full activation of p53.

In this study, we used phage display to identify a novel peptide that can inhibit p53 interactions with MDM2 (IC₅₀ = 10 nmol/L) and MDMX (IC₅₀ = 100 nmol/L) *in vitro*. Expression of a scaffold protein (thioredoxin) displaying this peptide sequence by recombinant adenovirus for the first time achieved disruption of both MDM2 and MDMX interaction with p53, resulting in efficient p53 activation and apoptosis of MDMX-overexpressing tumor cells in

Requests for reprints: Jiandong Chen, H. Lee Moffitt Cancer Center, MRC3057A, 12902 Magnolia Drive, Tampa, FL 33612. Phone: 813-903-6822; Fax: 813-903-6817; E-mail: Jiandong.chen@moffitt.org.

©2007 American Association for Cancer Research.
doi:10.1158/0008-5472.CAN-07-1140

culture and in mice in a p53-dependent fashion. These results show the advantage of targeting both MDM2 and MDMX for p53 activation and induction of apoptosis in cancer cells, and provide a novel structural motif for the design of potent p53 activators.

Materials and Methods

Phage display. An M13 phage library (Ph.D.-12, New England Biolabs) encoding random 12-mer peptides at the NH₂ terminus of pIII coat protein (2.7×10^9 sequences) was used. Glutathione *S*-transferase (GST)-MDM2-1-150 and GST-MDMX-1-200 fusion proteins containing the p53 binding domain of human MDM2 and MDMX were expressed in *E. coli* and loaded onto glutathione-agarose beads. The loaded beads were incubated with blocking buffer [0.1 mol/L NaHCO₃ (pH 8.6), 5 mg/mL bovine serum albumin (BSA), 0.02% NaN₃] for 1 h at 4°C, washed with TBST [50 mmol/L Tris (pH 7.5), 150 mmol/L NaCl, 0.1% Tween 20], and incubated in TBST at 4°C with 4×10^{10} phages. Bound phages were eluted with 0.2 mol/L glycine (pH 2.2), 1 mg/mL BSA and neutralized with 1 mol/L Tris (pH 9.1). The eluted phages were amplified as instructed by the manufacturer. The binding/amplification process was repeated for four cycles for both targets. Phage DNA was prepared and the region of interest was sequenced.

Fusion protein construction. *E. coli* thioredoxin was used as a scaffold to display structurally constrained peptides. Double-stranded oligonucleotide (5'-GTCCGCCTCTGAGTTTGACGTTTGTAGCATTATTGGCGCAGTTGACGTCGGAAAACG) encoding pDI was cloned into the RsrII site of pBAD/Thio vector (Invitrogen). The complete thioredoxin-coding region with the peptide insert was amplified by PCR (using 5'-GGTCGACCCATGGGATCTGATAAAATTATTCATC-3', 5'-GCTCGAGGGCCAGGTTAGCGTCG-3' primers), cleaved with *SalI* and *XhoI*, and cloned into pShuttle-IRES-hrGFP-1 vector (Stratagene). The plasmid was linearized with *PmeI* and cotransformed into *E. coli* BJ5183 with adenoviral backbone plasmid pAdEasy-1. Recombinant plasmids were linearized with *PacI* and transfected into AD-293 cells (Stratagene) to generate viruses. Recombinant adenoviruses were purified by ultracentrifugation on CsCl₂ gradients and titered using the Adeno-X Rapid Titer Kit (Clontech).

ELISA assay. GST-MDM2-1-150 and GST-MDMX-1-200 containing human MDM2 and MDMX, respectively, and His6-tagged human p53 expressed in *E. coli* were used in ELISA as previously described (30).

GST pull-down assay. ³⁵S[Methionine]-labeled MDMX and MDM2 were generated using the TNT *in vitro* transcription/translation kit (Promega). Five microliters of the translation products were mixed and incubated with glutathione-agarose beads loaded with 5 μg of GST-p53-1-52 in lysis buffer [50 mmol/L Tris-HCl (pH 8.0), 5 mmol/L EDTA, 150 mmol/L NaCl, 0.5% NP40, 1 mmol/L phenylmethylsulfonyl fluoride] for 2 h at 4°C. The beads were washed with lysis buffer, fractionated by SDS-PAGE, and bound MDMX and MDM2 were detected by autofluorography.

Cell lines and antibodies. Tumor cell lines H1299 (lung, p53-null), U2OS (bone), MCF-7 (breast), JEG-3 (placenta), and DLD-1 (breast) were maintained in DMEM with 10% fetal bovine serum. HCT116-p53^{+/+} and HCT116-p53^{-/-}

cells were kindly provided by Dr. Bert Vogelstein (Department of Oncology, Johns Hopkins University, Baltimore, MD); retinoblastoma Y79 cell line was provided by Dr. George Blanck (Department of Biochemistry, University of South Florida, Tampa, FL); and normal human foreskin fibroblasts were provided by Dr. Jack Pledger (Moffitt Cancer Center, Tampa, FL). A U2OS stable cell line with MDMX overexpression and U2OS stable cell line, expressing tetracycline-regulated human MDM2 and MDMX were previously described (14, 30). The following antibodies were used in the experiment: 3G9 (mouse) and a rabbit polyclonal serum for MDM2 Western blot and immunoprecipitation; DO-1 (PharMingen) and FL393 (Santa Cruz Biotechnology) for p53 Western blot; 8C6 monoclonal or a rabbit polyclonal serum for MDMX Western blot and immunoprecipitation; and anti-p21WAF (Santa Cruz Biotechnology) for p21. p53 ubiquitination assay was done as previously described (14).

Animal studies. Athymic-NCr-nu female mice, between 7 and 8 weeks of age, were inoculated s.c. on both flanks with 5×10^6 HCT116 cells. Tumor formation was followed for 4 to 6 days. When tumor size reached ~0.2 cm³, the mice were injected with 5×10^{10} plaque-forming units (pfu) of Ad-DI or control adenoviruses everyday for a total of five times. Tumor volume was calculated with the formula [(length + width) / 2]³ × 0.5236. Tumors recovered after termination of the experiments were fixed in formalin and paraffin sections were analyzed by immunohistochemical staining with rabbit antibodies against p53 and FLAG.

Results

Identification of a high-affinity MDM2 and MDMX binding peptide. To identify novel peptide inhibitors of MDM2 and MDMX, phage display was used to screen a 12-mer library to obtain peptides that bind to the p53-binding domains of MDM2 and MDMX. GST-MDM2 and GST-MDMX were used as baits and the binding/amplification process was repeated for four cycles for both targets. Phage DNA was prepared and the variable region was sequenced. The results showed that 7 of 10 MDMX-selected and 4 of 10 MDM2-selected phages contain the same insert (LTFEHYWAQLTS; Table 1). This peptide was named pDI for peptide dual inhibitor. The remaining phages contain unrelated and inactive sequences when tested by ELISA and were not further characterized.

The results above showed that screens using GST-MDM2 or GST-MDMX resulted in the selection of the same peptide. This suggests that pDI has such high affinity for both MDM2 and MDMX that it outcompeted any potential isoform-specific peptides by a significant margin. The pDI peptide (LTFEHYWAQLTS) is distinct from the p53 peptide (16-QETFSDLWKLPLP-28) and the previously identified 12/1 peptide (MPRFMDYWEGLN) that interacts with MDM2 and MDMX (33), but retains three key p53 hydrophobic residues (Phe¹⁹, Trp²³, and Leu²⁶, underlined) that contact the MDM2 pocket (34, 35). In an ELISA assay, pDI inhibited MDM2-p53 and MDMX-p53 interactions with IC₅₀ of 10

Table 1. Peptide sequences selected by phage display

MDMX selected phages	MDM2 selected phages
T-MX-1: F A P L N R T V E T S P	T-M2-1: Q Q M H L M S Y A P G P
T-MX-2: L T F E H Y W A Q L T S	T-M2-2: T I R P S T T M D S P T
T-MX-3: L T F E H Y W A Q L T S	T-M2-3: Y A N P Q M E K A F E S
T-MX-4: Y A V S S S P R V A A L	T-M2-4: L T F E H Y W A Q L T S
T-MX-5: L T F E H Y W A Q L T S	T-M2-5: L P N L T W A L M P G A
T-MX-6: L T F E H Y W A Q L T S	T-M2-6: Y A N P Q M E K A F A S
T-MX-7: L T F E H Y W A Q L T S	T-M2-7: L T F E H Y W A Q L T S
T-MX-8: L T F E H Y W A Q L T S	T-M2-8: L T F E H Y W A Q L T S
T-MX-9: V V H V P N S A T P P R	T-M2-9: L L A D T T H H R P W T
T-MX-10: L T F E H Y W A Q L T S	T-M2-10: L T F E H Y W A Q L T S

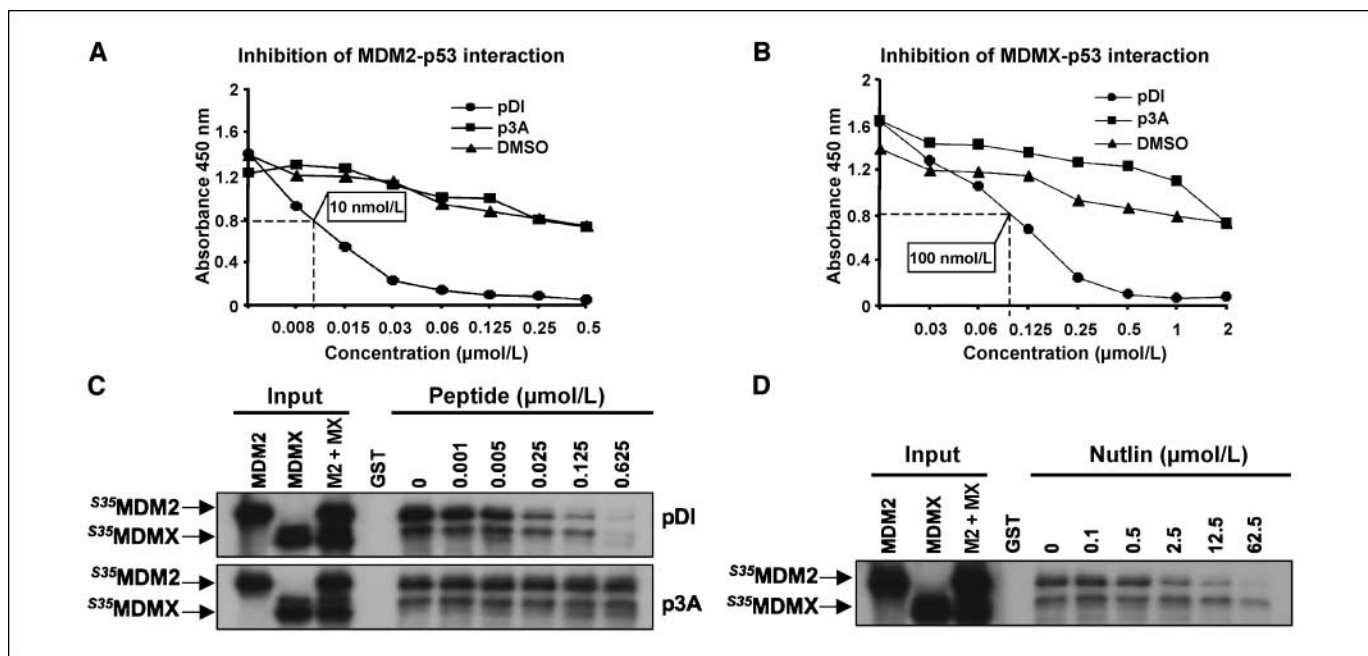


Figure 1. Disruption of MDM2 and MDMX-p53 interactions by a novel peptide. *A* and *B*, phage display-selected pDI and control p3A peptides were tested in an ELISA assay of GST-MDM2 and GST-MDMX binding to immobilized His6-p53. *C* and *D*, glutathione beads loaded with GST-p53-1-52 fusion protein were incubated with a mixture of *in vitro* translated MDM2 and MDMX and different concentrations of peptides or Nutlin. Binding of MDM2 and MDMX to GST-p53-1-52 in the presence of inhibitors was determined by autofluorography after washing and SDS-PAGE.

and 100 nmol/L respectively, which is 15-, 60-, and 300-fold better than 12/1, Nutlin, and p53 peptide on MDM2 (Fig. 1*A* and *B*; Table 2). Mutation of the three key hydrophobic residues to alanine (p3A) abrogated MDM2 and MDMX inhibition, suggesting that pDI mimics p53 binding to MDM2 and MDMX. In a different assay, pDI also inhibited GST-p53 capture of *in vitro* translated MDM2 and MDMX with different efficiency (Fig. 1*C*). In contrast, Nutlin only blocked MDM2 but had no effect on MDMX-p53 interaction (Fig. 1*D*). The 10-fold difference in IC_{50} for MDM2 and MDMX suggests that MDMX may bind p53 with higher affinity than MDM2, which is consistent with its mechanism of p53 inhibition by sequestration.

Construction of an MDM2 and MDMX inhibitory protein.

After unsuccessful attempts to activate p53 in cells by fusion or conjugation of pDI to the Antennapedia cell-permeable peptide, the pDI sequence was inserted into the active center of FLAG-tagged *E. coli* thioredoxin protein that serves as a display scaffold (ref. 36; Fig. 2*A*). Adenoviruses expressing the fusion proteins with wild-type pDI (Ad-DI) and control p3A (Ad-3A) sequences were constructed (Fig. 2*B*). The fusion proteins expressed in infected cells showed diffused cytoplasmic and nuclear staining, consistent with their small sizes (~15 kDa), and has a half life of ~1 h, which was unrelated to MDM2 binding (data not shown).

The pDI peptide was selected based on its ability to bind MDM2 and MDMX. To test whether insertion of pDI sequence into thioredoxin conferred the ability to binding MDM2 and MDMX, cells infected with Ad-DI virus were immunoprecipitated with FLAG antibody and analyzed for the coprecipitation of endogenous MDM2 and MDMX. The results showed that the FLAG-DI protein, but not FLAG-3A, coprecipitated with both MDM2 and MDMX when expressed in MCF-7 cells (Fig. 2*C*). Furthermore, FLAG-DI expression disrupted MDM2-p53 and MDMX-p53 coprecipitations (Fig. 2*D*). As expected, Nutlin failed to disrupt MDMX-p53 complex

in the same assay. Infection with Ad-DI did not cause p53 Ser¹⁵ phosphorylation (data not shown), suggesting that the fusion protein disrupted p53 binding to MDM2 and MDMX by a competitive mechanism without triggering DNA damage signaling. These results showed that the FLAG-DI fusion protein was expressed at levels sufficient to compete with p53 for binding to endogenous MDM2 and MDMX.

Activation of p53 by the MDM2 and MDMX inhibitory protein.

Disruption of MDM2-p53 and MDMX-p53 complexes should result in p53 stabilization and activation. As expected, infection of tumor cells or normal human foreskin fibroblasts expressing wild-type p53 with Ad-DI resulted in significant increase in p53 level and induction of p53 targets (p21, MDM2, and PUMA; Fig. 3*A* and *B*). The effects were not observed using Ad-3A or Ad-vector control viruses, indicating that they were dependent on the pDI sequence in the fusion protein. Infection of p53-null (HCT116-*p53*^{-/-}) or mutant (DLD1) cell lines failed to induce p53 target genes, indicating that the effect of Ad-DI was p53 dependent (Fig. 3*A* and *B*). Reverse transcription-PCR analysis showed that

Table 2. Inhibition of MDM2 and MDMX-p53 binding by peptides in ELISA

Peptides (compound)	Sequences	IC_{50} for MDM2 (μmol/L)	IC_{50} for MDMX (μmol/L)
p53pep	QETFSDLWKLPP	3.00	27.50
12/1	MPRFMDYWEGLN	0.15	1.25
Nutlin		0.60	No inhibition
pDI	LTFEHYWAQLTS	0.01	0.10
p3A	LTAEHYAAQATS	No inhibition	No inhibition

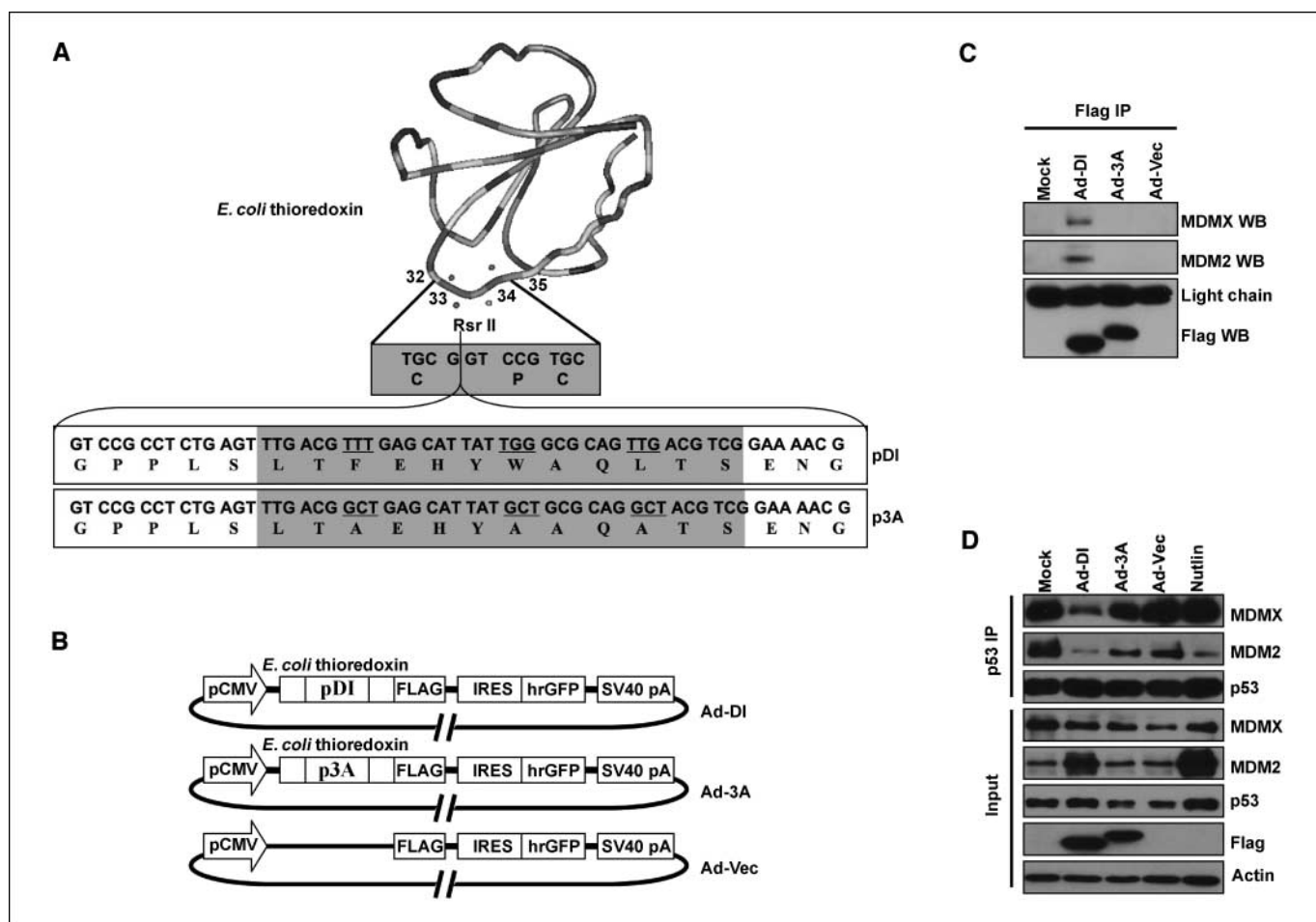


Figure 2. Design of recombinant adenovirus for expression of peptide epitopes. *A*, schematic representation of the scaffold protein *E. coli* thioredoxin with pDI and p3A inserted between Gly³³ and Pro³⁴ at the active center. *B*, the coding regions of thioredoxin-DI and thioredoxin-3A were fused to FLAG epitope in the adenovirus genome. The cytomegalovirus (CMV) promoter drives expression of FLAG-DI or FLAG-3A, and an internal ribosome entry site (IRES) element allows coexpression of hrGFP from the same transcript. *C*, MCF-7 cells were infected with Ad-DI, Ad-3A, and Ad-Vec (MOI, 300) for 48 h and cell lysate was immunoprecipitated with FLAG antibody and blotted for coprecipitation of MDM2 and MDMX. *D*, MCF-7 cells were treated with Ad-DI, Ad-3A, and Ad-Vec (MOI, 300) or Nutlin (10 μ mol/L) for 48 h and MG132 (30 μ mol/L) was added 4 h before harvest. Cell lysate was immunoprecipitated with p53 antibody and blotted for coprecipitation of MDM2 and MDMX.

the increase in p21 and MDM2 levels was associated with increase in mRNA (data not shown). Ad-DI infection also activated a stably integrated p53-responsive reporter, BP100-luc, in HCT116 and MCF-7 cells (Fig. 3C), indicating activation of p53 transcriptional function. Although FLAG-DI was diffusely localized to both nucleus and cytoplasm, MDM2 and p53 induced by its expression were predominantly nuclear. As expected, Ad-DI infection inhibited p53 ubiquitination by MDM2 (data not shown), consistent with its ability to disrupt MDM2-p53 binding. Cell cycle analysis by fluorescence-activated cell sorting (FACS) revealed an \sim 10-fold reduction of S-phase population in the Ad-DI-infected HCT116-*p53*^{+/+} cells but not in HCT116-*p53*^{-/-} cells (Fig. 3D). Ad-DI infection also induced significant apoptosis in HCT116-*p53*^{+/+} cells, but was much less effective in HCT116-*p53*^{-/-} cells (Fig. 3D). Therefore, the cell cycle arrest and apoptosis activities of Ad-DI are mediated by activation of p53.

Activation of p53 in cells overexpressing MDMX. Nutlin does not disrupt MDMX-p53 binding when applied at practical concentrations dictated by solubility and nonspecific toxicity (5–10 μ mol/L). Therefore, p53 activation by Nutlin is attenuated in cells overexpressing MDMX (30–32). To test whether Ad-DI is

more efficient in activating p53 in cells overexpressing MDMX, JEG3 (high MDM2 and MDMX) and Y79 (high MDMX) cells were treated with the virus (24, 28). The results showed that Ad-DI infection resulted in significant apoptosis in both cell lines, whereas Nutlin was less effective (Fig. 4A). These results suggested that FLAG-DI is able to overcome physiologic levels of MDM2 and MDMX overexpression.

To further test the ability of FLAG-DI in overcoming higher levels of MDM2 and MDMX overexpression, U2OS cells expressing tetracycline-regulated MDM2 (\sim 8 \times endogenous level) and MDMX (\sim 8 \times endogenous level) were treated with Ad-DI and Nutlin. The results showed that, as expected, Nutlin remained highly effective even when MDM2 is overexpressed, whereas MDMX overexpression completely abrogated the ability of Nutlin to activate p53 (Fig. 4B). In contrast, the activity of Ad-DI was only moderately inhibited by MDM2 and MDMX overexpression, consistent with a competitive mechanism of FLAG-DI action. Similar assay using U2OS overexpressing even higher levels of MDMX (30 \times endogenous level, noninducible) also showed the ability of Ad-DI to activate p53 under conditions when Nutlin was completely ineffective (data not shown). In addition, FACS

and 3-(4,5-dimethylthiazol-2-yl)-2,5-diphenyltetrazolium bromide (MTT) assays showed that Ad-DI induced significant apoptosis in U2OS-MDMX cells, which were completely resistant to Nutlin (Fig. 4C and D). Treatment of normal human foreskin fibroblasts with Ad-DI did not cause apoptosis (data not shown). This is expected because most nontransformed cell types do not undergo apoptosis on p53 activation (37). These results suggested that FLAG-DI is an efficient activator of p53 in tumor cells over-

expressing MDM2 and MDMX due to its ability to neutralize both proteins.

Antitumor effects of MDM2 and MDMX inhibition. To test the antitumor potential of Ad-DI, HCT116 tumor xenografts ($\sim 0.2 \text{ cm}^3$) were treated with daily single intratumoral (i.t.) injection of 5×10^{10} pfu Ad-DI or control virus for 5 consecutive days. This resulted in 90% suppression of tumor growth for the following 16 days by Ad-DI but not by control viruses or buffer (Fig. 5A). The differences in

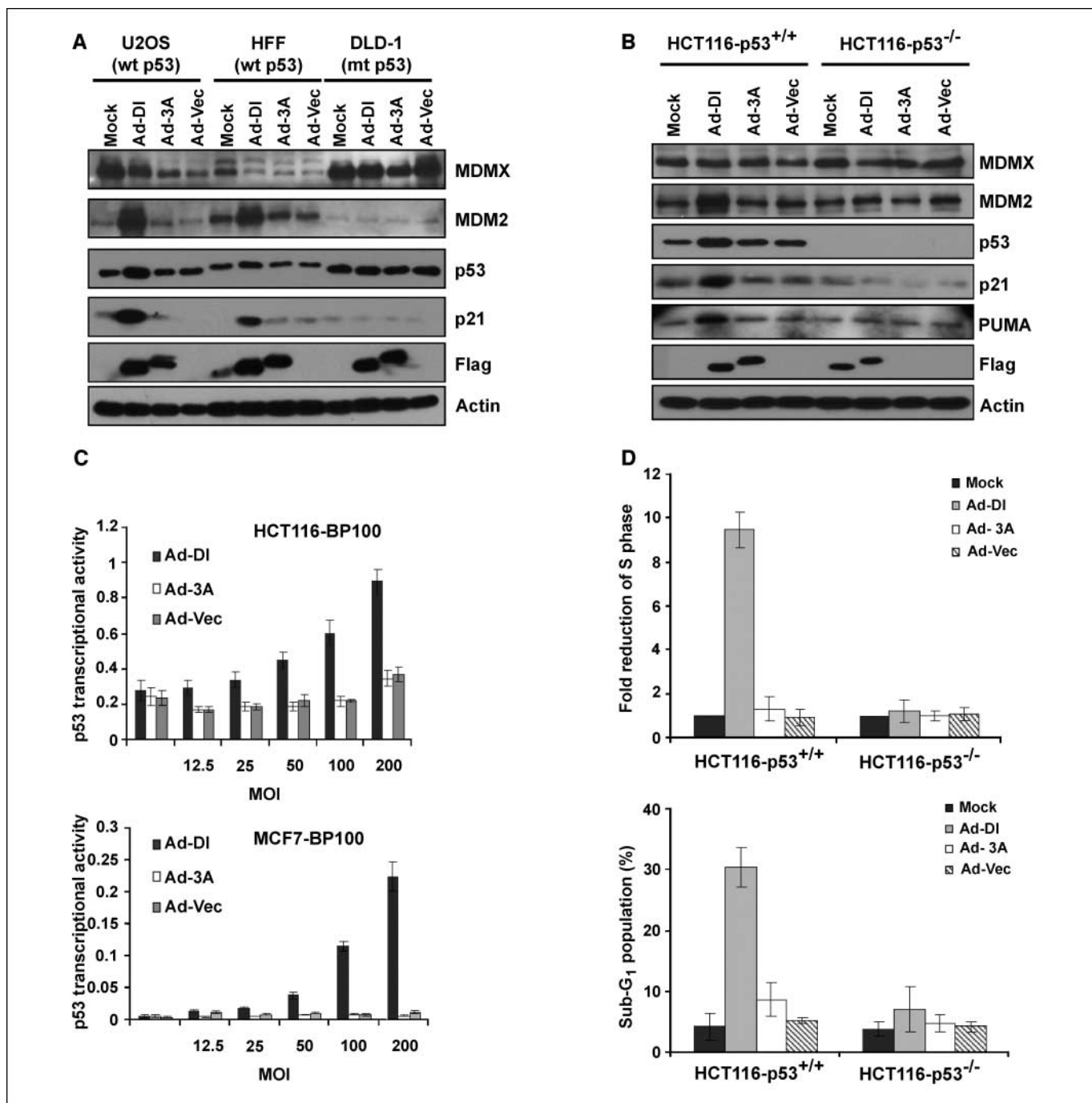


Figure 3. Inhibition of MDM2 and MDMX-p53 binding by FLAG-DI activates p53. *A* and *B*, cells were infected with the recombinant adenoviruses (MOI, 100) for 48 h and analyzed by Western blot. *C*, HCT116 and MCF-7 cells stably transfected with the p53-responsive reporter plasmid BP100-luc were infected with Ad-DI at the indicated MOI for 48 h and luciferase activity was determined ($n = 3$). *D*, HCT116-*p53*^{+/+} and HCT116-*p53*^{-/-} cells were infected with Ad-DI (MOI, 300) for 48 h. Reduction of S phase was analyzed by propidium iodide staining and FACS. Apoptosis was measured by the level of sub-G₁ fraction in FACS analysis.

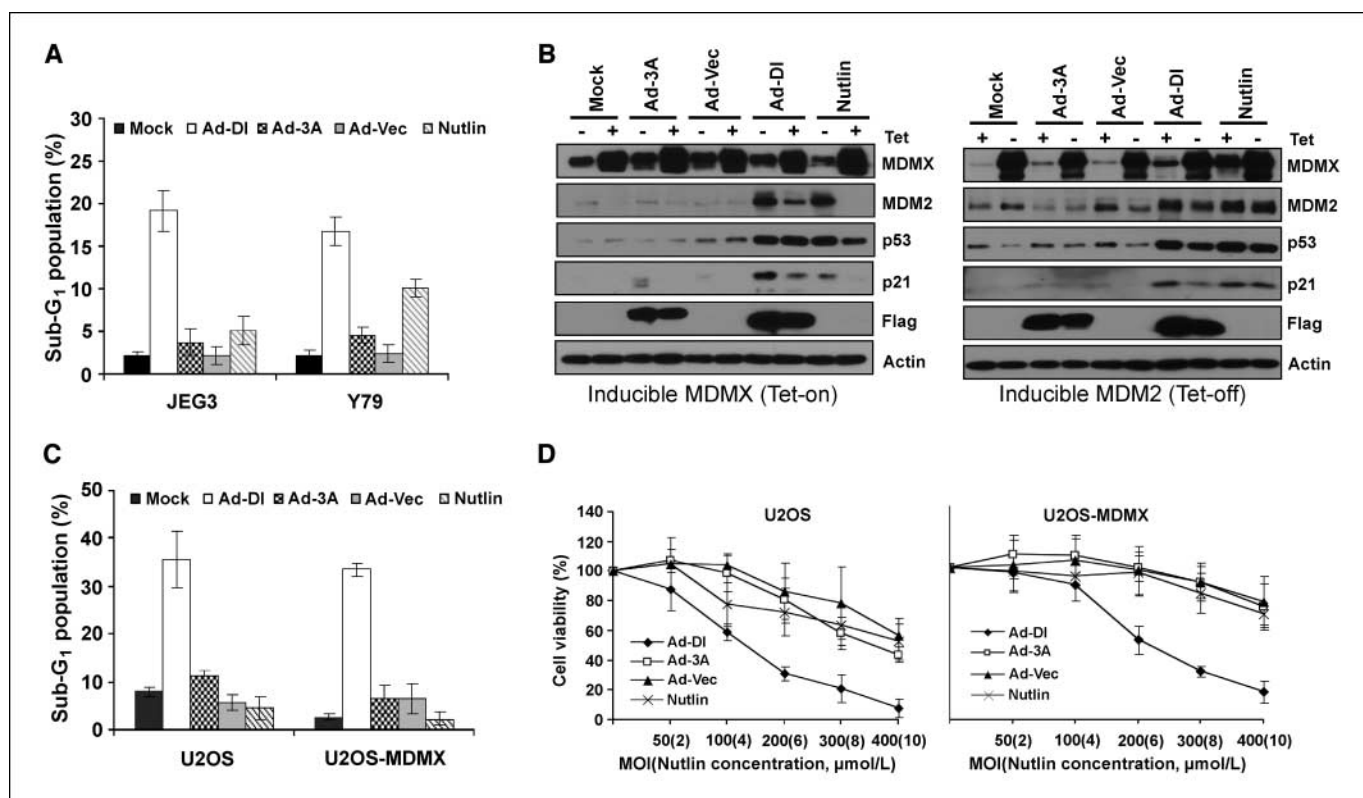


Figure 4. Activation of p53 by FLAG-DI in cells overexpressing MDM2 and MDMX. **A**, JEG3 and Y79 cells were treated with Ad-DI (MOI, 300) or Nutlin (10 $\mu\text{mol/L}$) for 48 h and analyzed by FACS for apoptotic sub-G₁ population. **B**, U2OS expressing inducible MDMX (Tet-on) and MDM2 (Tet-off) were treated with 0.1 $\mu\text{g/mL}$ tetracycline for 18 h, followed by treatment with Ad-DI (MOI, 100) or Nutlin (10 $\mu\text{mol/L}$) for additional 24 h, and p53 activation markers were analyzed by Western blot. **C**, U2OS and U2OS-MDMX cells were treated with Ad-DI (MOI, 300) and Nutlin (10 $\mu\text{mol/L}$) for 48 h and analyzed by FACS for sub-G₁ population. **D**, U2OS and U2OS-MDMX cells were treated with Ad-DI and Nutlin at indicated concentrations for 5 d and analyzed by MTT assay for cell viability.

tumor suppression effects of Ad-DI ($n = 10$), Ad-3A ($n = 6$), Ad-vector ($n = 8$), and buffer ($n = 17$) were statistically significant ($P < 0.01$). Similar treatment of larger tumors ($>0.5 \text{ cm}^3$) resulted in moderate growth inhibition in only a subset of animals (data not shown), most likely due to limited access of the virus to distant parts of the tumor. Strong induction of p53, MDM2, and p21 was observed in the extract of tumors 48 h after injection with Ad-DI (Fig. 5B). Immunohistochemical staining of tumor serial sections showed localized expression of FLAG-DI in the nucleus and cytoplasm of tumor cells near the sites of injection, which correlates with significant p53 staining in the same area (Fig. 5C).

Consistent with cell culture results, the antitumor effect of Ad-DI was strictly dependent on p53. The growth of HCT116-*p53*^{-/-} tumor xenograft was not inhibited by Ad-DI ($n = 6$) and Ad-3A ($n = 6$, $P > 0.05$; Fig. 5D). Furthermore, Ad-DI also inhibited the growth of tumor xenograft formed by a modified HCT116-MDMX cell line overexpressing MDMX (~ 5 -fold; Fig. 5D; ref. 24; $P < 0.01$, $n = 5$) and induced p53 activation, as determined by Western blot and immunohistochemical staining (data not shown). Ad-DI and control viruses were well tolerated in mice after i.t. administration, with no observable weight loss or pathologic changes of different organs (data not shown).

Discussion

Recent studies suggest that MDM2 regulates p53 mainly by promoting its degradation, whereas MDMX acts by sequestration of p53 (38, 39). Although current understanding of the role of

MDMX in cancer is still limited, cell culture experiments suggest that MDMX is a significant player in suppressing p53 activity in at least a subset of tumors. Several studies of MDMX expression in clinical samples also strongly implicate its involvement in cancer development. These observations suggest a need to further evaluate the potential of MDMX as a therapeutic target. Currently, the most attractive approach for targeting MDMX is to use small molecules to disrupt MDMX-p53 association. MDMX knockout and RNAi provided valuable evidence for the functional importance of MDMX in regulating p53. However, because MDMX also interacts with other molecules such as MDM2 and casein kinase 1, MDMX depletion does not provide the best simulation of disrupting MDMX-p53 binding.

The MDM2 inhibitor Nutlin was developed specifically for MDM2 (40, 41). Interestingly, we and others showed that Nutlin is at least 30-fold less efficient in disrupting MDMX-p53 binding (30–32). When applied at practical concentrations, Nutlin is likely to function only by inhibiting MDM2. MDMX is also insensitive to a class of small-molecule MDM2 inhibitors that are α -helical mimics based on the terphenyl scaffold (42).¹ These observations suggest that the p53-binding pockets on MDM2 and MDMX have differences that affect the binding of small molecules. Such differences may also compromise the effect of other small molecules optimized for MDM2.

¹ B. Hu and J. Chen, unpublished results.

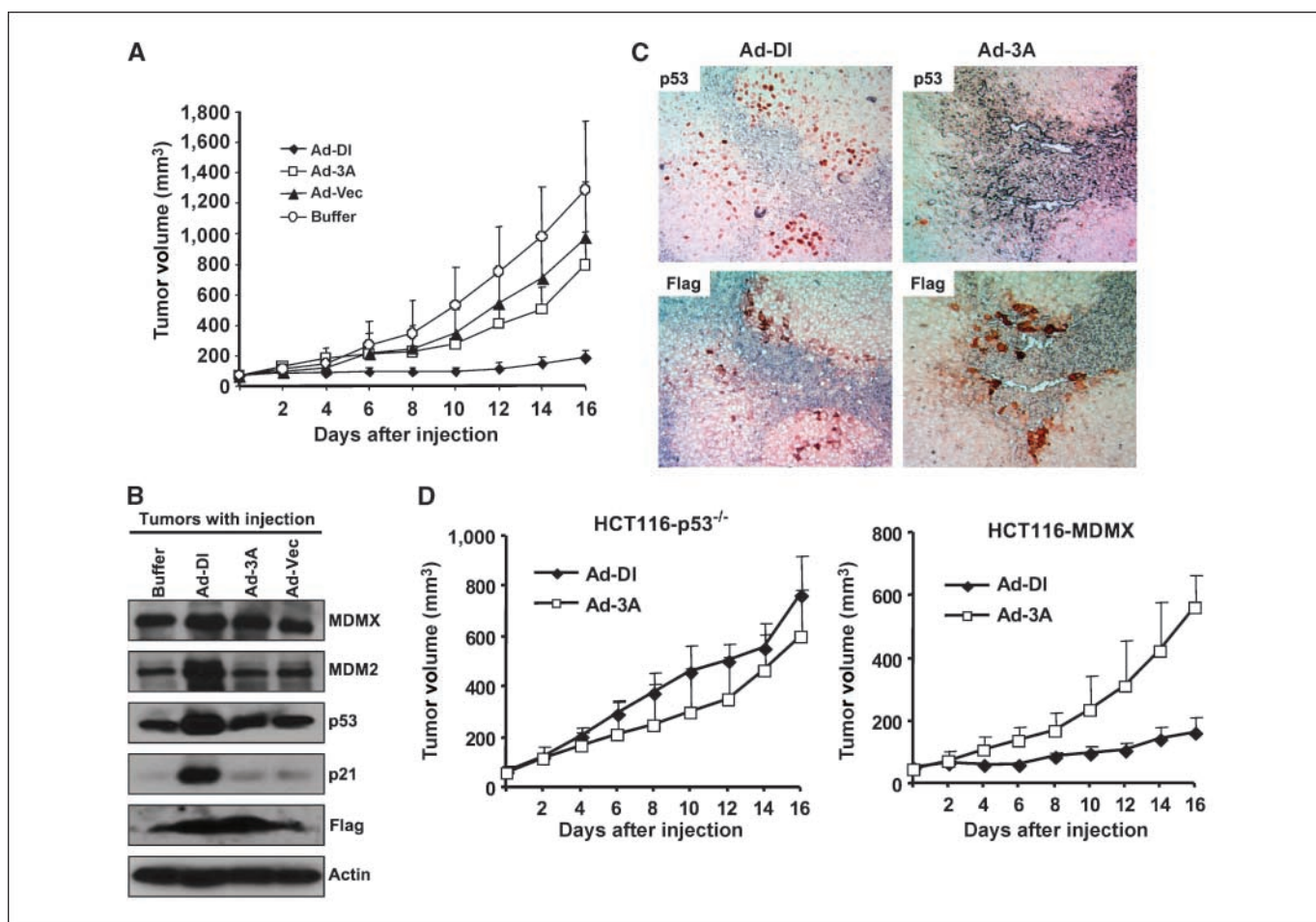


Figure 5. Antitumor activity of Ad-DI. *A*, nude mice bearing HCT116-*p53*^{+/+} xenografts were treated with Ad-DI, Ad-3A, Ad-vector, or buffer by daily i.t. injections (5×10^{10} pfu/injection) for 5 consecutive days. The tumor volumes were measured every 2 d after completion of treatment cycle. *B*, representative tumor samples recovered 48 h after injection were analyzed by Western blot. *C*, representative tumor specimens 48 h after injection with Ad-DI and Ad-3A were stained for p53 and FLAG in serial sections. *D*, HCT116-*p53*^{-/-} and HCT116-MDMX tumor xenografts were treated with i.t. injection of 5×10^{10} Ad-DI or Ad-3A for 5 consecutive days. Tumor growth was measured for the indicated time frame after completion of injections.

For therapeutic applications, it is beneficial to have an inhibitor that is dual-specific for MDM2 and MDMX. Our attempts to screen for MDM2 and MDMX binding peptides in this study resulted in the identification of the same sequence motif. This finding suggests that MDM2 and MDMX have similar binding specificity to peptide sequences, which is distinct from their interactions with small molecules. It is possible that peptides rely on extensive contacts with the p53 binding pockets and is not sensitive to minor differences that affect small-molecule ligands. Interestingly, in both ELISA and GST pull-down assays, disruption of MDMX-p53 interaction always requires ~ 10 -fold higher concentrations of the pDI peptide. This suggests that MDMX may bind p53 with higher affinity than MDM2, which is consistent with its mechanism of p53 inhibition by forming stable complexes.

Our results showed that simultaneous inhibition of MDM2 and MDMX binding to p53 has strong proapoptotic potential in cell culture and can efficiently suppress tumor growth *in vivo*. The ability of Ad-DI to induce apoptosis is a significant contrast to Nutlin, which induces cell cycle arrest in most tumor cell lines (41). It is possible that the ability of FLAG-DI to target both MDM2 and MDMX caused p53 activation over the apoptotic

threshold. These results provide a proof-of-principle for the antitumor potential of MDM2/MDMX dual inhibitors. The potent pDI peptide also provides a novel motif for structural study of MDM2 and MDMX interactions with a high-affinity ligand and should aid the design of small-molecule inhibitors. Cancer therapy using the Ad-DI virus may be limited by the efficiency of delivery to large tumors. However, it is possible that gene therapy is a useful approach against certain tumors such as retinoblastoma, 60% of which overexpress MDMX (28). In such cases, the small tumor sizes, enclosed environment, and a need to avoid genotoxicity and preserve vision may make it a potential therapeutic option (43).

Acknowledgments

Received 4/10/2007; revised 5/31/2007; accepted 7/2/2007.

Grant support: NIH (J. Chen).

The costs of publication of this article were defrayed in part by the payment of page charges. This article must therefore be hereby marked *advertisement* in accordance with 18 U.S.C. Section 1734 solely to indicate this fact.

We thank the Moffitt Molecular Biology, Flow Cytology, and Tissue Cores for DNA sequencing, FACS analyses, and processing of histologic samples.

References

1. Wu X, Bayle JH, Olson D, Levine AJ. The p53-mdm-2 autoregulatory feedback loop. *Genes Dev* 1993;7:1126-32.
2. Levine AJ. p53, the cellular gatekeeper for growth and division. *Cell* 1997;88:323-31.
3. Chen J, Wu X, Lin J, Levine AJ. mdm-2 inhibits the G₁ arrest and apoptosis functions of the p53 tumor suppressor protein. *Mol Cell Biol* 1996;16:2445-52.
4. Bond GL, Hu W, Levine AJ. MDM2 is a central node in the p53 pathway: 12 years and counting. *Curr Cancer Drug Targets* 2005;5:3-8.
5. Shvarts A, Steegenga WT, Riteco N, et al. MDMX: a novel p53-binding protein with some functional properties of MDM2. *EMBO J* 1996;15:5349-57.
6. Jones SN, Roe AE, Donehower LA, Bradley A. Rescue of embryonic lethality in Mdm2-deficient mice by absence of p53. *Nature* 1995;378:206-8.
7. Montes de Oca Luna R, Wagner DS, Lozano G. Rescue of early embryonic lethality in mdm2-deficient mice by deletion of p53. *Nature* 1995;378:203-6.
8. Parant J, Chavez-Reyes A, Little NA, et al. Rescue of embryonic lethality in Mdm4-null mice by loss of Trp53 suggests a nonoverlapping pathway with MDM2 to regulate p53. *Nat Genet* 2001;29:92-5.
9. Stad R, Little NA, Xirodimas DP, et al. Mdmx stabilizes p53 and Mdm2 via two distinct mechanisms. *EMBO Rep* 2001;2:1029-34.
10. Tanimura S, Ohtsuka S, Mitsui K, Shirouzu K, Yoshimura A, Ohtsubo M. MDM2 interacts with MDMX through their RING finger domains. *FEBS Lett* 1999;447:5-9.
11. Sharp DA, Kratowicz SA, Sank MJ, George DL. Stabilization of the MDM2 oncoprotein by interaction with the structurally related MDMX protein. *J Biol Chem* 1999;274:38189-96.
12. Linares LK, Hengstermann A, Ciechanover A, Muller S, Scheffner M. HdmX stimulates Hdm2-mediated ubiquitination and degradation of p53. *Proc Natl Acad Sci U S A* 2003;100:12009-14.
13. Gu J, Kawai H, Nie L, et al. Mutual dependence of MDM2 and MDMX in their functional inactivation of p53. *J Biol Chem* 2002;277:19251-4.
14. Pan Y, Chen J. MDM2 promotes ubiquitination and degradation of MDMX. *Mol Cell Biol* 2003;23:5113-21.
15. Kawai H, Wiederschain D, Kitao H, Stuart J, Tsai KK, Yuan ZM. DNA damage-induced MDMX degradation is mediated by MDM2. *J Biol Chem* 2003;278:45946-53.
16. de Graaf P, Little NA, Ramos YF, Meulmeester E, Letteboer SJ, Jochemsen AG. Hdmx protein stability is regulated by the ubiquitin ligase activity of Mdm2. *J Biol Chem* 2003;278:38315-24.
17. Chen L, Li C, Pan Y, Chen J. Regulation of MDMX-p53 interaction by casein kinase 1 α . *Mol Cell Biol* 2005;25:6509-20.
18. Okamoto K, Kashima K, Pereg Y, et al. DNA damage-induced phosphorylation of MdmX at serine 367 activates p53 by targeting MdmX for Mdm2-dependent degradation. *Mol Cell Biol* 2005;25:9608-20.
19. LeBron C, Chen L, Gilkes DM, Chen J. Regulation of MDMX nuclear import and degradation by Chk2 and 14-3-3. *EMBO J* 2006;25:1196-206.
20. Pereg Y, Lam S, Teunisse A, et al. Differential roles of ATM- and Chk2-mediated phosphorylations of Hdmx in response to DNA damage. *Mol Cell Biol* 2006;26:6819-31.
21. Zhang Y, Wolf GW, Bhat K, et al. Ribosomal protein L11 negatively regulates oncoprotein MDM2 and mediates a p53-dependent ribosomal-stress checkpoint pathway. *Mol Cell Biol* 2003;23:8902-12.
22. Bhat KP, Itahana K, Jin A, Zhang Y. Essential role of ribosomal protein L11 in mediating growth inhibition-induced p53 activation. *EMBO J* 2004;23:2402-12.
23. Lohrum MA, Ludwig RL, Kubbutat MH, Hanlon M, Vousden KH. Regulation of HDM2 activity by the ribosomal protein L11. *Cancer Cell* 2003;3:577-87.
24. Gilkes DM, Chen L, Chen J. MDMX regulation of p53 response to ribosomal stress. *EMBO J* 2006;25:5614-25.
25. Ramos YF, Stad R, Attema J, Peltenburg LT, van der Eb AJ, Jochemsen AG. Aberrant expression of HDMX proteins in tumor cells correlates with wild-type p53. *Cancer Res* 2001;61:1839-42.
26. Danovi D, Meulmeester E, Pasini D, et al. Amplification of Mdmx (or Mdm4) directly contributes to tumor formation by inhibiting p53 tumor suppressor activity. *Mol Cell Biol* 2004;24:5835-43.
27. Riemenschneider MJ, Buschges R, Wolter M, et al. Amplification and overexpression of the MDM4 (MDMX) gene from 1q32 in a subset of malignant gliomas without TP53 mutation or MDM2 amplification. *Cancer Res* 1999;59:6091-6.
28. Laurie NA, Donovan SL, Shih CS, et al. Inactivation of the p53 pathway in retinoblastoma. *Nature* 2006;444:61-6.
29. Vassilev LT, Vu BT, Graves B, et al. *In vivo* activation of the p53 pathway by small-molecule antagonists of MDM2. *Science* 2004;303:844-8.
30. Hu B, Gilkes DM, Farooqi B, Sebti SM, Chen J. MDMX overexpression prevents p53 activation by the MDM2 inhibitor Nutlin. *J Biol Chem* 2006;281:33030-5.
31. Patton JT, Mayo LD, Singhi AD, Gudkov AV, Stark GR, Jackson MW. Levels of HdmX expression dictate the sensitivity of normal and transformed cells to Nutlin-3. *Cancer Res* 2006;66:3169-76.
32. Wade M, Wong ET, Tang M, Stommel JM, Wahl GM. Hdmx modulates the outcome of p53 activation in human tumor cells. *J Biol Chem* 2006;281:33036-44.
33. Bottger V, Bottger A, Howard SF, et al. Identification of novel mdm2 binding peptides by phage display. *Oncogene* 1996;13:2141-7.
34. Bottger V, Bottger A, Garcia-Echeverria C, et al. Comparative study of the p53-2 and MDMX-p53 interfaces. *Oncogene* 1999;18:189-99.
35. Kussie PH, Gorina S, Marechal V, et al. Structure of the MDM2 oncoprotein bound to the p53 tumor suppressor transactivation domain. *Science* 1996;274:948-53.
36. Bottger A, Bottger V, Sparks A, Liu WL, Howard SF, Lane DP. Design of a synthetic Mdm2-binding mini protein that activates the p53 response *in vivo*. *Curr Biol* 1997;7:860-9.
37. Ringshausen I, O'Shea CC, Finch AJ, Swigart LB, Evan GI. Mdm2 is critically and continuously required to suppress lethal p53 activity *in vivo*. *Cancer Cell* 2006;10:501-14.
38. Franco S, Froment P, Bogaerts S, et al. Mdm4 and Mdm2 cooperate to inhibit p53 activity in proliferating and quiescent cells *in vivo*. *Proc Natl Acad Sci U S A* 2006;103:3232-7.
39. Toledo F, Krummel KA, Lee CJ, et al. A mouse p53 mutant lacking the proline-rich domain rescues Mdm4 deficiency and provides insight into the Mdm2-4-p53 regulatory network. *Cancer Cell* 2006;9:273-85.
40. Vassilev LT. Small-molecule antagonists of p53-2 binding: research tools and potential therapeutics. *Cell Cycle* 2004;3:419-21.
41. Tovar C, Rosinski J, Filipovic Z, et al. Small-molecule MDM2 antagonists reveal aberrant p53 signaling in cancer: implications for therapy. *Proc Natl Acad Sci U S A* 2006;103:1888-93.
42. Chen L, Yin H, Farooqi B, Sebti S, Hamilton AD, Chen J. p53 α -Helix mimetics antagonize p53/MDM2 interaction and activate p53. *Mol Cancer Ther* 2005;4:1019-25.
43. Balmer A, Zografos L, Munier F. Diagnosis and current management of retinoblastoma. *Oncogene* 2006;25:5341-9.

Cancer Research

The Journal of Cancer Research (1916–1930) | The American Journal of Cancer (1931–1940)

Efficient p53 Activation and Apoptosis by Simultaneous Disruption of Binding to MDM2 and MDMX

Baoli Hu, Daniele M. Gilkes and Jiandong Chen

Cancer Res 2007;67:8810-8817.

Updated version Access the most recent version of this article at:
<http://cancerres.aacrjournals.org/content/67/18/8810>

Cited articles This article cites 43 articles, 25 of which you can access for free at:
<http://cancerres.aacrjournals.org/content/67/18/8810.full#ref-list-1>

Citing articles This article has been cited by 15 HighWire-hosted articles. Access the articles at:
<http://cancerres.aacrjournals.org/content/67/18/8810.full#related-urls>

E-mail alerts [Sign up to receive free email-alerts](#) related to this article or journal.

Reprints and Subscriptions To order reprints of this article or to subscribe to the journal, contact the AACR Publications Department at pubs@aacr.org.

Permissions To request permission to re-use all or part of this article, use this link
<http://cancerres.aacrjournals.org/content/67/18/8810>.
Click on "Request Permissions" which will take you to the Copyright Clearance Center's (CCC) Rightslink site.